Method for the correlation coefficient estimation of the bottom echo signal in the shallow water application using interferometric echo sounder

Piotr GRALL[1], Jacek MARSZAL[1]

Corresponding author: Piotr GRALL, email: piograll@pg.edu.pl

[1] Gdańsk University of Technology, Faculty of Electronics, Telecommunications and Informatics, Department of Sonar Systems, Narutowicza 11/12, 80-233 Gdańsk, Poland

Abstract The article presents a new method for the assessment of bottom echo correlation coefficient in the presence of multiple echoes. Bottom correlation coefficient is a parameter that characterizes spatial properties of echo signal. Large variability of the bottom shape or properties (for example caused by the presence of bottom objects) and the presence of the acoustic shadow strongly influence the value of the correlation coefficient. There is a problem, however, in the proper determination of correlation coefficient of the bottom echo when more than one echo is present. In the shallow water application, the echoes coming to the hydroacoustic array from various directions influence the measured value of the correlation coefficient. The method proposed by the authors challenges this issue by applying a subarray processing based on the initial depth estimation. The article presents the preliminary research results and describes the limitations of the proposed method.

Keywords: coherence estimation, multiphase echo sounder, sub-array processing

1. Introduction

The multiphase echo sounder is a device which operation is based on high-resolution methods [1-3]. Using only a small set of receive elements it resolves the number and direction of echoes generated in response to the probing signal. Received samples (snapshots) are used to form a proper model equation and subsequently this equation is solved using various linear algebra methods. Each high-resolution method uses slightly different approach to obtain the solution of model equation but many of them require prior estimation of the number of signals present [4]. This number is used to perform subspace separation which then allows using various subspace properties to obtain the desired solution [5-6].

The value of correlation coefficient modulus, between any pair of the receive elements, is determined by the properties of the bottom and the geometrical relations between the footprint and the receive array, and the probing signal length [7-8]. In the case of a deep mount over a flat bottom, when the echo sounder array is situated far away from the water surface, bottom coherence coefficient changes gradually (Figs. 1a, b). The mean value of the correlation coefficient reflects the combined effect of the baseline decorrelation, shifting footprint and noise. These effects can be easily simulated. Simulation examples presented in this article were calculated using methodology similar to the one presented in the Ref. [3]. The single ping values also exhibits local perturbations from the mean value due to the random nature of the backscattered echo signal. Once the array is situated in the shallow water the value of the coherence coefficient is strongly affected by multiple echoes coming to the receive array at the same time (Figs. 1c, b). The complex structure of the echoes in the real environment introduces even more variability to the correlation coefficient value (Fig. 2).

If an object is present on the bottom it introduces disturbance in the correlation coefficient value due to the presence of the acoustic shadow and changes in the bottom geometry (Fig. 3) [9]. Once additional echoes are present the bottom image is distorted, especially for larger ranges (Fig. 3b) [10]. Proper processing is required to recover the bottom correlation coefficient values. The aim of the proposed new method is to spatially filter the signal acquired in the shallow water scenario (Fig. 3) to extract the bottom echo reflection

correlation coefficient as if the additional echoes were not present (i.e. to obtain values similar to the ones depicted in Fig. 1b).
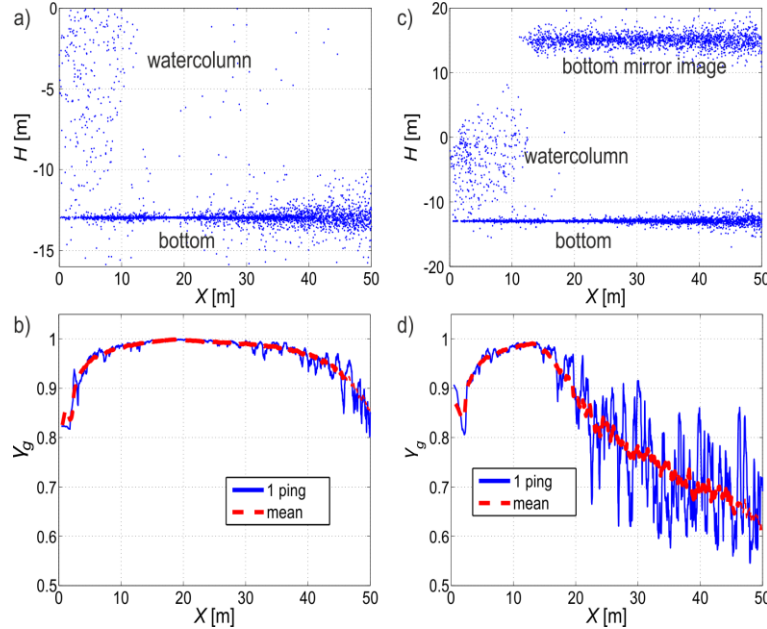

Fig. 1. Simulated data correlation coefficient example: a) simple bottom configuration for 1 echo at H=-13 m, b) correlation coefficient for 1 echo. (blue – single ping, red – mean of 50 pings), c) simple bottom configuration for 2 echoes at H=-13 m and H=15 m (draft of the array is assumed to be 1 meter) d) correlation coefficient for 2 echoes. (blue – single ping, red – mean of 50 pings).
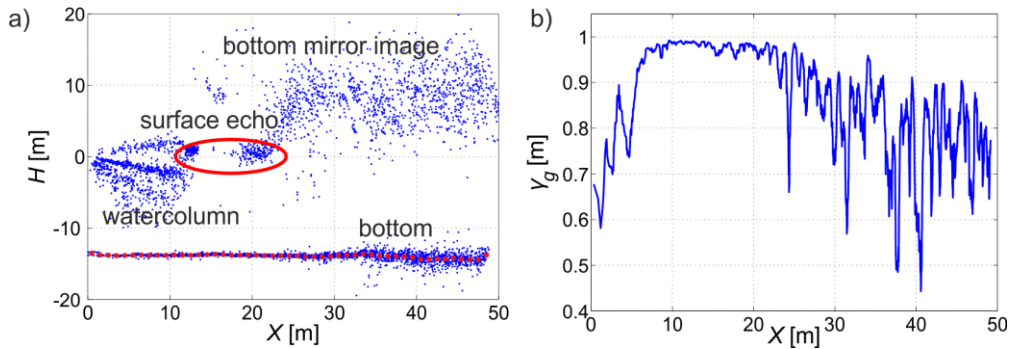

Fig. 2. Real data correlation coefficient example: a) complex echo structure. red dots – bottom generalization using 1 meter bin size, blue dots – resolved echoes sources, b) correlation coefficient – single ping.

2. Correlation coefficient estimation

Using few assumptions the echo model for interferometric echo sounder can be formulated as [11]:

$$s(n) = \sum_{i=1}^{M} a_i \, e^{(\alpha_i + j \, u_i) \, d \, n} + w(n), \tag{1a}$$

$$a_i = A_i e^{j\Theta_i}, \; u_i = k \sin \theta_i \; , k = \frac{2\pi}{\lambda}, \lambda = \frac{c}{f}, n = 0, 1, 2, \dots, N-1. \tag{1b}$$

where $s(n)$ is the received signal at a given hydrophone at a given time instant (time dependence in Eq. (1a) is omitted for clarity reasons), a_i is the complex signal amplitude at the reference receive element

(n=0, Fig. 4c), u_i is the acoustic wavenumber, λ is the wavelength at the probing signal frequency f, α_i is the exponential damping factor (its value for $f = 500$ kHz equals approx. 0.2 dB/m, i.e. 0.023 1/m and for practical applications is usually omitted in the echo model formulation [1, 3]), d is the inter-element spacing, $w(n)$ is additive noise at each array element, N is the number of the receive elements, M is the number of echoes and θ_i is the direction to the echo respective to the receive array main response axis.
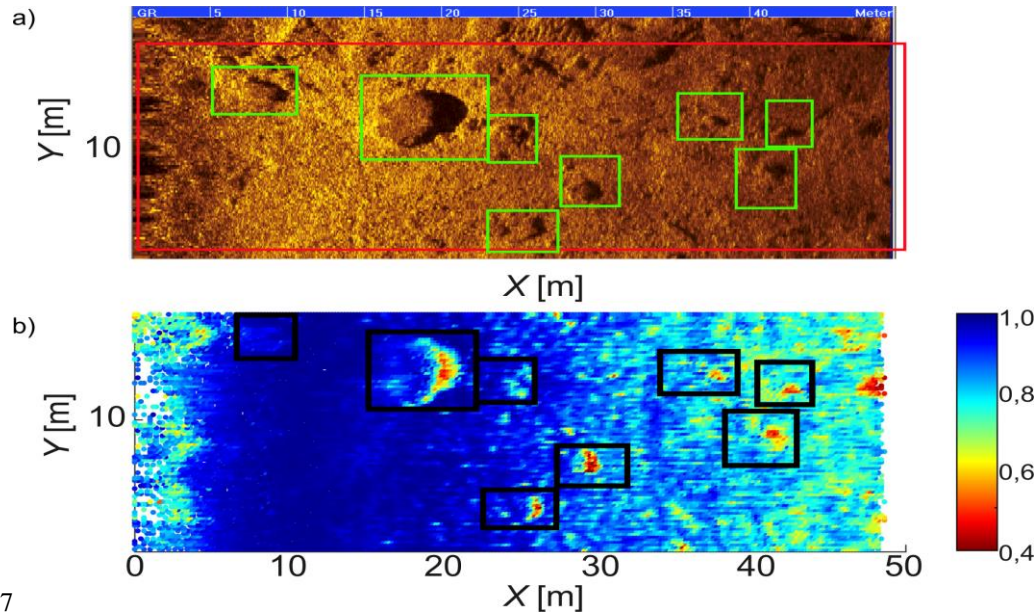

Fig. 3. Unprocessed bottom image example: a) side-scan sonar image. Shadow casting objects are indicated in green boxes, b) corresponding correlation coefficient spatial distribution (color-coded). Each colour dot represent bottom patch of 0.2 x 0.2 meters.

In the case of a deep mount, when only one echo signal is present (M=1), complex correlation coefficient values between each two elements $\gamma_{i,j}$ can be estimated from the following formula:

$$\gamma(t)_{i,j} = \frac{\text{cov}(\mathbf{A_0}(*,i),\mathbf{A_0}(*,j))}{\sqrt{\text{var}(\mathbf{A_0}(*,i))\ \text{var}(\mathbf{A_0}(*,j))}}, \tag{2}$$

where i and j are the numbers of the receive elements and $\mathbf{A_0}$ is k x N matrix of k subsequent snapshots (sets of N signal samples) of the received signal, as described by the Eq. (1a), The snapshots are cantered around the time sample for the time t. The number of time samples should be large enough to remove the effect of noise on the estimated value, but at the same time small enough so its value represents local bottom properties perturbations. The global correlation coefficient γ_g can be defined as the average modulus value of all the possible combinations of element pairs:

$$\gamma_g(t) \stackrel{df}{=} \frac{2}{N(N-1)} \sum_{i=2}^{N} \sum_{j=1}^{i-1} |\gamma(t)_{i,j}|. \tag{3}$$

Real data example presented in the article is based on the data acquired by the EgdeTech 6205 multiphase echo sounder. The device utilizes two 10 element receive arrays with $d \approx 0.5\lambda$ at frequency 500 kHz, and allows recording of the complex signal after matched filter processing. For the range of 50 meters it generates 4340 complex envelope time samples (see Ref. [12] for more details). The recorded signals were processed using Eqs. (2) and (3) to generate Figs. 2b and 3b. Figure 3b presents problems with bottom features detection based on the correlation coefficient value distribution in the shallow water application. Once bottom mirror echo appears ($M{\neq}1$) the correlation coefficient value is heavily distorted. The values change between 1 and 0 obscuring the bottom objects (right half of Fig. 3b).

3. Bottom echo correlation coefficient estimation

Now we would like to recover the correlation coefficient of the bottom echo in the presence of multiple echoes. To overcome the problem stated in the Sect. 1 the received signals needs to be post-processed. Firstly, the low resolution bottom image is obtained (Figs. 2a and 4a). Resolved bottom echo samples are filtered and binned. The bin size is equal to 1 m in the horizontal direction. Bottom samples depth for each bin are averaged. The bottom generalization is required to obtain smooth steering angles estimates. Single snapshot angle estimates would be less accurate for steering due to the large depth variability of bottom samples (see Figs. 1 and 2), which is well-known feature of raw multiphase bottom estimates. Based on the obtained bin coordinate pairs (X, H)-horizontal distance and depth, low resolution steering angles couples (R, θ) are calculated (Fig. 4a):

$$R = \sqrt{X^2 + H^2} = \frac{ct}{2}, \tag{4a}$$

$$\theta = \beta - \psi = \arctan\left(\frac{H}{X}\right) - \psi, \tag{4b}$$

where R is the slant range, β is the bottom grazing angle (in relation to the horizontal), ψ is the main array response axis tilt angle. The steering angles for each time sample are interpolated between the low resolution steering angles using time-distance equivalence indicated in Eq. (4a). The steering is only calculated for $R>13$ m (Fig. 4b) i.e. for ranges greater than vertical distance to the first bottom return.
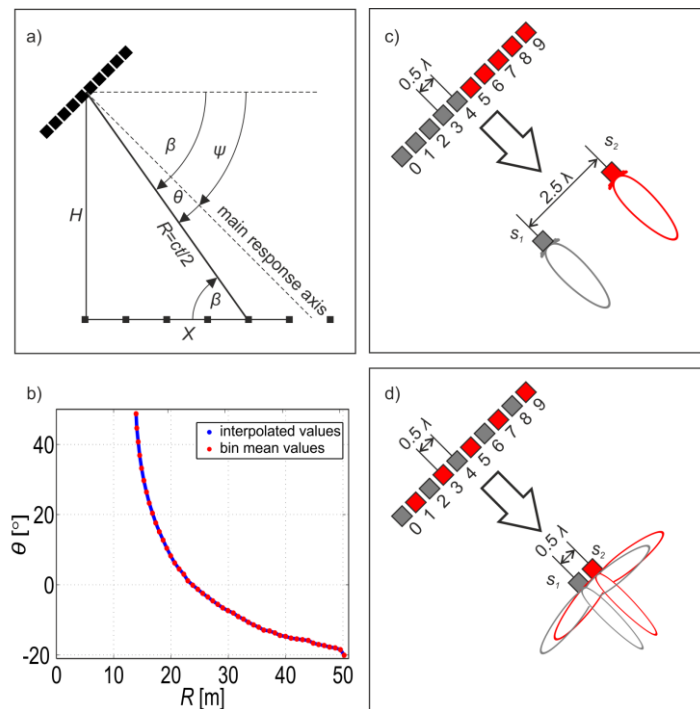

Fig. 4. Processing steps: a) calculation of the low-resolution steering angles, b) interpolation of the low resolution steering angles to the time/range samples, c) case I subarray beamforming, d) case II subarray beamforming.

Now the 10 element array is divided into subarrays and each consists of 5 elements. In the case I, the arrays are not overlapping each other (Fig. 4c). The subarray size equals 2λ and the arrays centres are separated by 2.5λ. In the case II, the arrays are overlapping (Fig. 4d). The subarray size equals 4λ and the arrays centres are separated by 0.5λ. The signals form the sub-arrays are than dynamically beamformed using the previously calculated steering angles. Assuming $d = 0.5\lambda$ and $\alpha = 0$ (i.e. constant signal envelope for a single snapshot), signals from subarray elements can be coherently summed [13]:

$$s_{1,2} = \sum_{k=1}^{5} s(n_k) \ e^{-j\pi \sin\theta \ n_k}, \tag{5}$$

where n_k are ordinal numbers of elements forming the subarrays $s_{1,2}$ (depending on the case, see Figs. 4c and 4d). The exponential factor compensates the inter-element phase delay of the echo signal. For the case I, the main lobe beamwidth equals approximately 35° and no grating lobes are present. For the case II, the main lobe beamwidth equals approximately 17°, but very large grating lobe appears for angles larger than ±60° (even without any steering applied).

The correlation coefficient modulus values for each time sample is estimated using Eqs. (2) and (3) for subarray outputs. The number of time samples k chosen in presented example is 31 which is equivalent to 0.4 m of flat bottom for the edge of observation range. Subsequently, correlation coefficient values are mapped to each bottom sample at given X. Finally, correlation coefficient values are averaged using 0.2 bins and gathered in the 2D image.

4. Results

The overall effect of dynamic beam forming is presented in Fig. 5. Both cases significantly reduced the spatial variability of the correlation coefficient value due to the reduction of the influence of the undesired echoes. The first case allows extracting a more detailed image of bottom features then the second case. It is especially noticeable for the large bottom object at X=20 m and smaller bottom (vaguely visible in the second variant and in the initial unprocessed image) object at X=8 m. Differences in the sensitivity between both variants are caused mainly by the different separation of the subarrays, and the absence or presence of the grating lobes. The grating lobe influence is visible in the vertical wavy pattern at X=17 m in Fig. 5b. For X<5 m there is also a difficulty region caused by rapid changes of the correlation coefficient values due to the baseline decorrelation effect [8].
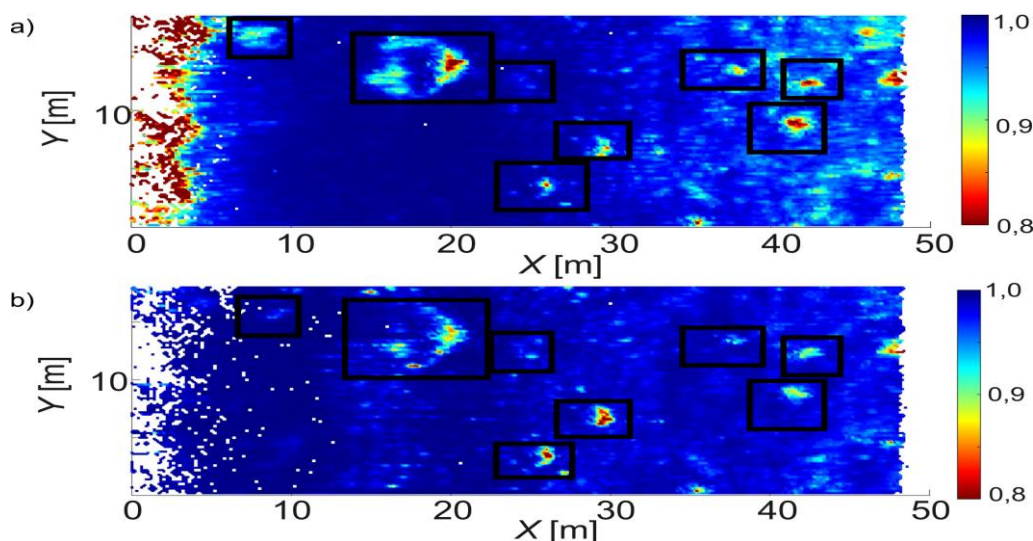

Fig. 5. Processing results. Spatial distribution of bottom echo signal correlation coefficient modulus: a) case I, b) case II.

There are several advantages of the proposed method for bottom object detection over traditional side scan sonar image analysis. The correlation coefficient value is normalized between 0 and 1 and its values are not affected by sonar image enhancement methods such as time varied gain and histogram equalization. Thanks to this feature the obtained image might be used for manual or computer aided bottom features detection. The correlation coefficient spatial distribution image is much simplified in comparison to sonar image but retains the key image features – locations of acoustic shadows and rapid changes in bottom geometry. The main limitation of this method is caused by the wide beamwidth of the main lobe of the subarrays. It limits the range of the applicability of the proposed method, as for large distances the angular separation between bottom and mirror bottom echoes diminishes and both echoes might be simultaneously present within the main lobe of the steered subarrays. For the studied example the angular separation for range 50 m equals approx. 30°, which is less than half of the beamwidth, and the mirror bottom echo can be properly filtered. Additionally same small objects might not be detected due to the applied spatial

binning (such as the object at X =22, Y= 12 – Fig. 5). Another limitation of the proposed method is caused by the bottom shape. For non-flat or very rough bottom with large vertical extensions, spatial filtering might not be effective due bottom features overlay (two close echoes within the main lobe).

5. Conclusions

The presented method enables the extraction of the bottom echo correlation coefficient in the shallow water environment. The application of the low resolution subarray beamforming removes the influence of the echoes form the undesired directions. In result, a simplified image of the bottom is obtained which can be used for manual or automatic bottom object detection. The method operation range is limited by the echoes spatial distribution and the main lobe beamwidth. In the studied bottom sample, the non-overlapping sub-arrays perform better than overlapping due to larger spatial separation and the absence of the grating lobes. Further studies will be performed to fine tune the processing algorithm.

Additional information

The authors declare no competing financial interests.

References

1. P.H. Kraeutner, J.S. Bird. Principal components array processing for swath acoustic mapping. Proc. of Oceans'97, 1246-1254, 1997. DOI: 10.1109/OCEANS.1997.624174
2. P.H. Kraeutner, J.S. Bird. Beyond interferometry, resolving multiple angles-of-arrival in swath bathymetric imaging. Proc. of Oceans'99, 37-45, 1999. DOI: 10.1109/OCEANS.1999.799704
3. P.H. Kraeutner, J.S. Bird, B. Charbonneau, D. Bishop, F. Hegg. Multi-angle swath bathymetry sidescan quantitative performance analysis. Proc. of Oceans'02, 2253–2263, 2002. DOI: 10.1109/OCEANS.2002.1191981
4. P. Grall, J. Marszal, Theoretical analysis of a new approach to order determination for a modified Prony method in swath mapping application. Hydroacoustics, 20:63-74, 2017.
5. B.D. Rao, K.S. Arun. Model based processing of signals: a state space approach. Proc. of the IEEE, 80(2): 283-309, 1992. DOI: 10.1109/5.123298
6. A.-J. van der Veen, E.F. Deprettere, A.L. Swindlehurst. Subspace-based signal analysis using singular value decomposition, Proc. of the IEEE, 81(9):1277-1308, 1993. DOI: 10.1109/5.237536
7. X. Lurton. Swath bathymetry using phase difference: theoretical analysis of acoustical measurement precision, IEEE Journal of Oceanic Engineering, 25(3):351–363, 2000. DOI: 10.1109/48.855385
8. G. Jin, D. Tang. Uncertainties of differential phase estimation associated with interferometric sonars, IEEE Journal of Oceanic Engineering, 21(1):53-64, 1996. DOI: 10.1109/48.485201
9. T. G Michael, B. Marchand, J.D. Tucker, T.M. Marston, D. D. Sternlicht, M. R. Azimi-Sadjadi. Image-Based Automated Change Detection for Synthetic Aperture Sonar by Multistage Coregistration and Canonical Correlation Analysis, 41(3), 2015. DOI: 10.1109/JOE.2015.2465631
10. Ø. Midtgaard, T.O. Saebo, R.E. Hansen, Estimation of detection/classification performance using interferometric sonar coherence, Proceedings of 3rd International Conference on Underwater Acoustic Measurements (UAM), Greece, 2009.
11. P. Grall, I. Kochanska, J. Marszal. Direction-of-Arrival Estimation Methods in Interferometric Echo Sounding. Sensors, 20:3556, 2020. DOI: 10.3390/s20123556
12. P. Grall, J. Marszal, Depth determination accuracy of the modified Prony method in a swath mapping application, IEEE 2018 Joint Conference – Acoustics, 74-79, 2018. DOI: 10.1109/ACOUSTICS.2018.8502328
13. H.L. Van Trees, Optimum Array Processing Part IV of Detection, Estimation, and Modulation Theory, Wiley & Sons, New York, 2002.